Dynamics of Cyanide Binding to Ferrous *Scapharca inaequivalvis* Homodimeric Hemoglobin†

Alberto Boffi* and Emilia Chiancone

CNR Center of Molecular Biology and Department of Biochemical Sciences, University La Sapienza, 00185 Rome, Italy

Eric S. Peterson, Jiaqian Wang, Denis L. Rousseau, and Joel M. Friedman

Department of Physiology and Biophysics, Albert Einstein College of Medicine, Bronx, New York 10461

Received July 30, 1996; Revised Manuscript Received December 5, 1996⊗

ABSTRACT: Flash photolysis experiments have been carried out for the first time on a hemoglobin ferrous cyanide adduct with an 8 ns laser pulse. A 95% nonexponential rebinding process occurs within 2 μs after full photolysis in ferrous cyanide dimeric *Scapharca inaequivalvis* hemoglobin (HbI), indicating that once photolyzed the cyanide anion is not able to escape from the protein matrix and rebinds to the heme iron. The resonance Raman spectrum of the 10 ns photoproduct is identical to that of the fully relaxed deoxy derivative, indicating that in the ferrous cyanide HbI adduct protein relaxation occurs within 10 ns after photolysis. This behavior is at variance with that of the carbonmonoxy HbI derivative in which very little geminate rebinding is observed and the photoproduct relaxes with a lifetime of 1 μs. The fast relaxation of the cyanide HbI photoproduct can be accounted for by the small perturbation of the heme structure induced by cyanide binding to ferrous HbI. This is consistent with a deoxy-like conformation of the HbI ferrous cyanide adduct and implies that the pathway for relaxation involves only minor local rearrangements of the heme moiety. Photolysis experiments carried out on ferrous cyanide horse myoglobin, which can be saturated only partially, show a qualitatively similar behavior in ligand rebinding, indicating that the geminate process of the cyanide anion is a general phenomenon in hemoproteins.

Ligand rebinding to heme proteins after photolysis is a complex phenomenon since the photolyzed ligand encounters several energy barriers which determine the reaction pathway leading to ligand escape from the protein or to recombination with the iron atom. Several multistep mechanisms have been proposed to account for the observed kinetic behavior after photolysis at room temperature. The linear three-step model is one of the most widely used and has been applied to a number of different proteins and various ligands (Austin et al., 1975; Morris & Gibson, 1980; Henry et al., 1983; Gibson et al., 1986; Gibson, 1989). The overall reaction scheme is

$$A \underset{k_2}{\overset{k_1 + k_{h\nu}}{\leftrightarrows}} B \underset{k_4}{\overset{k_3}{\leftrightarrows}} C \underset{k_6}{\overset{k_5}{\leftrightarrows}} D$$

where A is the heme protein with the ligand bound, B its photodissociated state where the ligand is still within the heme pocket, C represents an intermediate species in which the ligand is embedded in the protein matrix, and D is the final dissociation product in which the ligand is in the solvent phase. In the framework of this scheme, to interpret the kinetics of the geminate rebinding process, a set of constraints must be assumed in order to obtain plausible values of the six rate constants: (i) the solutions must be consistent with the observed overall rate of ligand association and dissociation obtained in conventional mixing experiments, (ii) the scheme must describe all phenomena involved in the passage of the ligand from the iron to the solvent, and (iii) the relaxation of the protein from its photodissociated state to the deoxy state has to be taken into account as also this process may contribute to the overall observed signal.

Previous studies of geminate rebinding in *Scapharca inaequivalvis* hemoglobin (HbI) have been carried out with CO, NO, O_2, and isonitriles (Chiancone & Gibson, 1989; Chiancone et al., 1993) both in the nanosecond and picosecond time scales. A faster geminate recombination rate, k_2, was obtained for NO ($t_{1/2}$ = 7 ps) and O_2 ($t_{1/2}$ = 10 ps), with respect to Mb, while the values of k_4 and k_5 were in the same range as in all other heme proteins investigated (Chiancone et al., 1989). In the case of CO, a very small (5%) geminate component was observed, as in most heme proteins. In comparison, isonitriles exhibit 90% ligand rebinding within a few hundred picoseconds (Chiancone et al., 1989). The relaxation of the HbI−CO photoproduct to the deoxy derivative has been investigated in transient resonance Raman and optical absorption experiments in the nanosecond to millisecond time scale (Rousseau et al., 1993; Chiancone et al., 1993). These studies have revealed that it occurs with a lifetime of about 1 μs and involves large rearrangements in the heme group peripheral interactions and a small change in the iron−proximal histidine linkage.

Recently, a complete kinetic, thermodynamic, and spectroscopic characterization of the ferrous cyanide HbI derivative has been carried out (Boffi et al., 1996). These studies revealed that in HbI at pH 9.2 the ferrous cyanide adduct is unusually stable (K_{assoc} =17 M^{-1}) with respect to other hemoglobins and myoglobins (K_{assoc} = 2.5 M^{-1}), that the binding process is noncooperative (n = 0.96), and that the stability is determined mainly by a slow overall dissociation rate constant. The current mechanistic ideas on the cyanide dissociation reaction from the ferrous derivative are based

† Work supported in part through National Institutes of Health Grant GM 44343 and the W. M. Keck Foundation to J.M.F.

* Corresponding author. Fax: 39-6-44 40 062.

⊗ Abstract published in *Advance ACS Abstracts,* March 1, 1997.

S0006-2960(96)01889-2 CCC: $14.00

on the assumptions that the cyanide anion must be protonated in order to enter the protein matrix from either the heme pocket or the solvent and that it must release the proton within the heme pocket in order to bind to the iron atom (Bellelli et al., 1990; Brunori et al., 1992). Moreover, to explain the pH dependence of the rate of cyanide dissociation in a number of heme proteins, it has been proposed that the distal histidine may act as the proton source/sink in the transient protonation of cyanide (Bellelli et al., 1990; Brancaccio et al., 1994; Dou et al., 1996). These observations prompted the present investigation on the photoproduct relaxation of the ferrous cyanide HbI adduct in order to gain information on the true rate-limiting steps of this complex reaction mechanism. The relaxation process was followed by means of flash photolysis and transient resonance Raman experiments. In addition, since the current mechanistic ideas on the cyanide binding reaction to ferrous heme proteins are based on the behavior of myoglobin, the relaxation of the ferrous cyanide horse myoglobin photoproduct was characterized by flash photolysis; the transient resonance Raman study was precluded by the low degree of saturation that can be attained even at high cyanide concentrations.

MATERIALS AND METHODS

The dimeric hemoglobin from *S. inaequivalvis* was extracted and purified as described previously (Chiancone et al., 1981). Horse heart myoglobin was obtained from Sigma (St. Louis, MO) and filtered before use. Ferrous cyanide hemoglobin derivatives were prepared by adding a 200 μL aliquot of a concentrated 2 M stock solution of KCN in a 0.1 M, pH 9.2 borate buffer to a 500 μL aliquot of protein solution resulting in a ratio of approximately 500:1 of CN^- to heme. CO derivatives were prepared from oxygen-bound hemoglobin solutions by passing CO gas over the surface of a 100 μL aliquot in a sealed vial. Deoxy derivatives were prepared by passing N_2 over an oxyhemoglobin sample and then adding 5 equiv of sodium dithionite. All samples were approximately 0.5 mM in heme for the flash photolysis experiments and approximately 1 mM in heme for the resonance Raman experiments. The samples were then loaded under a nitrogen atmosphere into sample cells with either a 200 or 500 μm pathlength (Hellma P/N 124-QS, Jamaica, NY). The quartz front window of the Raman cell was replaced with a sapphire window, which yielded a flatter baseline in the low-frequency region of the spectrum. The sample cell was mounted in a custom-made brass holder, which was cooled to approximately 10 °C and rotated fast enough such that a new sample volume was interrogated with each laser shot. Photoproduct buildup and artifacts from sample spinning were found to be negligible by varying the spinning rate and by taking visible absorption spectra before and after each experiment. This sample preparation and arrangement was used for both the Raman and flash photolysis experiments.

Flash photolysis experiments were carried out on the ferrous cyanide HbI and horse heart Mb derivatives at 20 °C. The flash photolysis apparatus used for the rebinding rate studies utilized the doubled output of a Nd:YAG laser at 532 nm (Continuum Surelite, Santa Clara, CA) to photolyze the samples and the continuous wave (cw) output of a HeCd laser at 441.6 nm (Liconix P/N 4230NB, Santa Clara, CA) to monitor the recombination via changes in sample absorbance. The photolysis pulse was 8 ns in duration and was focused to a diameter of approximately 2 mm on the sample with an 800 mm lens. To achieve 100% photolysis within the illuminated sample volume, the photolysis pulse energy was increased until the amplitude of the signal was saturated, typically requiring approximately 2 mJ per pulse. The unfocused HeCd laser probe beam passed through the sample collinear with the Nd:YAG beam, was spectrally separated from the 532 nm light using a colored glass filter (BG-12, Schott Glass Technologies Inc. Durjea, PA), a dichroic mirror (CVI, Putnam, CT), and a single monochromator (Varian P/N AA-5, Palo Alto, CA), and was measured with a photomultiplier tube as the detector (Hamamatsu P/N R928, Bridgewater, NJ). The detector output was digitized by a 500 MHz oscilloscope (LeCroy P/N 7200 with a 7242B timebase/sampling head, Chestnut Ridge, NJ). Each sample file contained 50 000 points separated by 10 ns. Traces for 100 laser shots were averaged. Identical results were obtained from running the laser at 10 Hz and slowly spinning the sample and by running the laser at 1 Hz and not spinning the sample. The data were converted from transmission to change in absorption by taking a logarithm, subtracting a baseline, and normalizing.

Fitting of the recombination kinetics was carried out according to a simplified two-step linear scheme (including only species A, B, and C). The intrinsic rate of bond disruption, k_1, was set to zero since the overall dissociation rate (involving k_1, k_3, and k_5) as measured in a conventional stopped-flow measurement was found to be 0.011 s^{-1} (Boffi et al., 1996) and as such does not contribute significantly on the time scale of the recombination kinetics (Brunori et al., 1992). The initial condition at 10 ns, the end of the laser pulse, was 97% of the population in state B and 3% in state A. The 3×3 rate constant matrix was iteratively diagonalized to yield the observed rates k_2, k_3, and k_4 (eigenvalues) and corresponding amplitudes (eigenvectors) which best fit the experimental time course. A phenomenological two-exponential fit was also attempted but gave a poor fit in that the fast phase, accounting for the first 200 ns in HbI and 50 ns in Mb, was clearly biased. Data fitting was performed on a 486 PC using Matlab (Matlab Inc. Natick, MA).

Visible time-resolved resonance Raman spectra on the HbI−CN ferrous derivative were recorded at 10 °C. These spectra were obtained using an 8 ns, 435.8 nm pulse to both photodissociate the ligand and probe the Raman spectrum. The laser used was a Nd:YAG laser (Continuum NY81C-20, Santa Clara, CA), which produced 450 mJ pulses at 20 Hz in the second harmonic output at 532 nm. About 4 W of the 532 nm beam was focused into a homemade 90 cm long cell filled with 120 psi of hydrogen to Raman shift the laser to 435.8 nm. Neutral density filters were used to reduce the energy of the 435.8 nm pulses to 100 μJ, and these were focused at an incidence angle of 45° with a 150 mm plano-convex lens to an approximately 300 μm diameter spot on the sample. The Raman scattered light was collected at normal incidence to the sample (135° to the laser) with a 50 mm Nikon F/1.4 camera lens and focused with an *f*-matching lens onto the 50 μm $\times$ 5 mm slit of a 0.64 m single monochromator using an 1800 grooves/mm grating (ISA HR640, Metuchen, NJ). The Rayleigh line was reduced in intensity with a holographic notch filter (Kaiser P/N HNF-1171 centered at 442 nm, Ann Arbor, MI), and a depolarizer (CVI P/N DPL-10, Putnam, CT) was used to scramble the polarization of the collected light and thus eliminate intensity artifacts created by polarization-dependent grating reflectivity. The detector was an intensified diode array run in the

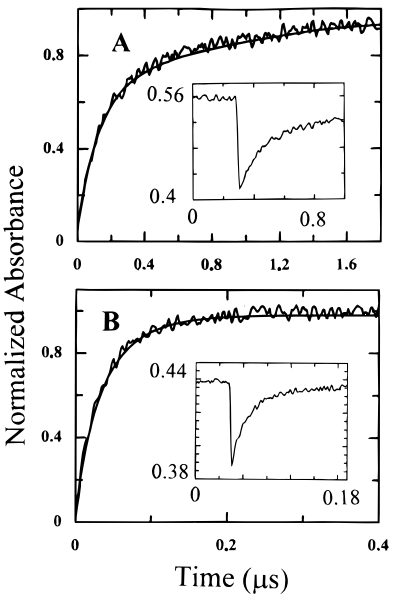

FIGURE 1: Flash photolysis data for (A) ferrous cyanide HbI and (B) ferrous cyanide horse heart Mb. The protein concentration was 250 μM in 0.1 M borate buffer, pH 9.2, containing 0.5 M KCN and approximately 2 mM dithionite. The cell path length was 500 μm. The experimental data are shown together with the fitted curves. The insets show the fast phase of the kinetics on a shorter time scale; the absorbance values of the inset are not normalized.

cw mode (Princeton Instruments P/N IRY-1024S/B, Trenton, NJ). The total accumulation time per spectrum was 30 min. The spectral bandwidth of the monochromator was approximately 2.5 cm^{-1}, and the discretization on the detector face was approximately 0.9 cm^{-1} per pixel. Raman spectra were calibrated using a toluene spectrum with previously determined peak assignments. A least squares fit was used to map pixel number into relative wavenumbers. The Raman spectra were baseline corrected using a polynomial fitting routine in LabCalc (Galactic Industries, Salem, NH).

RESULTS

Flash photolysis experiments were carried out in parallel on ferrous cyanide HbI and horse heart myoglobin (Mb) at pH 9.2 (Figure 1). After photolysis, a large decrease in absorbance is observed at 442 nm that recovers within 2 μs in HbI and within 0.5 μs in Mb. The observed absorbance changes are clearly nonexponential and correspond to ligand recombination after full photolysis. The percent photolysis achieved was estimated to be greater than 97% as calculated from the sample concentration and the difference in extinction coefficients at 442 nm measured in the cw absorption spectra (Figure 2). The smaller amplitude observed in the case of Mb (Figure 1B) is due to incomplete cyanide saturation at 0.5 M cyanide (Keilin & Hartree, 1955) . The data in Figure 1 were fitted according to the scheme detailed under Materials and Methods. The rate constants are reported in Table 1, and the relative contributions of species A, B, and C to the total signal are plotted as a function of time in Figure 3.

The resonance Raman spectra of the 10 ns photoproducts for ferrous HbI−CN and HbI−CO are shown in Figure 4 along with the spectrum of the deoxy derivative measured in parallel, all at pH 9.2. The spectra of the 10 ns HbI−CN photoproduct and of the deoxy derivative at pH 9.2 are perfectly superimposable with each other and also with the cw Raman spectrum measured previously at pH 7.0 (Rousseau et al., 1993).

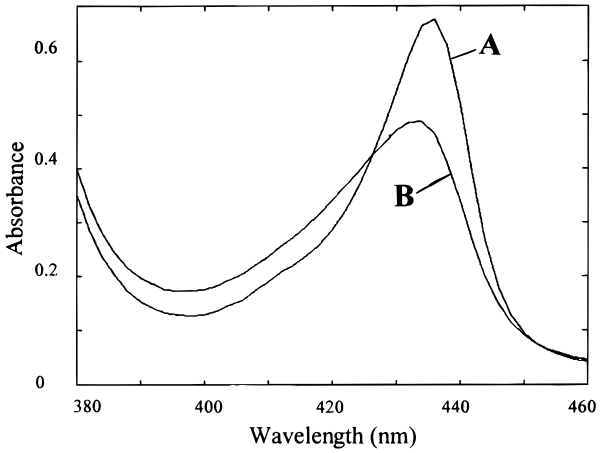

FIGURE 2: Absorption spectra of (A) ferrous cyanide and (B) deoxy HbI. The spectra were measured under the same conditiions as in Figure 1.

Table 1: Rate Constants for Cyanide Rebinding to HbI and Horse Heart Mb after Photolysis[a]

protein	k_2	k_3	k_4
HbI−CN	2.4	3.3	0.94
Mb−CN	26	6	0.96

[a] The fits were carried out according to the procedure outlined under Materials and Methods. The rate constants are expressed in μs^{-1}.

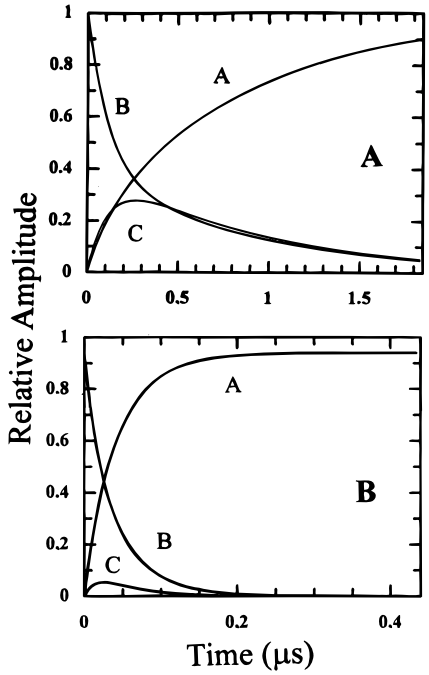

FIGURE 3: Relative contributions of species A, B, and C to the total transient absorption signal in Figure 1 as a function of time generated using the parameters listed in Table 1. Panels: (A) ferrous cyanide HbI; (B) ferrous cyanide Mb. For a description of the species, see the text.

DISCUSSION

The large fraction of geminate recombination observed in the ferrous cyanide HbI and Mb adducts is an unexpected result on the basis of the current interpretation of cyanide binding to ferrous heme proteins. The photolability of the complex under continuous illumination indicates a high quantum yield, comparable to that measured in the carbonmonoxy heme protein derivatives (Keilin & Hartree, 1955). In addition, as is the case with CO, the overall dissociation

rate of cyanide from ferrous hemoglobins and myoglobins is slow (0.1−0.01 s^{-1}), a finding attributed to the high activation energy required to break the iron−carbon bond (Brunori et al., 1992; Reddy et al., 1996). However, the presence of a large geminate recombination in ferrous cyanide HbI and Mb reported in this work taken together with the low iron−carbon bond energy for CN^- (Boffi et al., accompanying paper) calls for a reinterpretation of the cyanide binding reaction to ferrous heme proteins.

From a qualitative point of view, the nanosecond geminate process observed in ferrous cyanide HbI and Mb is strongly reminiscent of the behavior of bulky isonitriles, although the kinetics are faster for the isonitriles than for cyanide (Reisberg & Olson, 1980; Chiancone & Gibson, 1989). *tert*-Butylisonitrile, in particular, shows monophasic recombination kinetics which account for more than 90% of the total signal. In this case, the obvious explanation is that the bulky *tert*-butyl group is unable to escape from the pocket after photolysis due to steric constraints, which results in complete recombination of the photolyzed ligand. Similarly, in the case of the ferrous cyanide adduct, the high geminate yield indicates that the photolyzed ligand is not able to overcome the barrier through the protein matrix and exit to the solvent presumably because of its charge. In addition, the slow rebinding kinetics may indicate that the cyanide transiently binds to a site in the protein before moving back into the heme pocket and rebinding to the iron.

A quantitative description of the overall binding process, however, requires further considerations. In the analysis only the first two steps in the kinetic scheme will be addressed. In fact, the protein/solvent partition equilibrium (step III) cannot be determined unambiguously due to the presence of the cyanide protonation equilibrium (see below). Fitting of the recombination data was carried out according to the procedure outlined under Materials and Methods to yield unique values for the constants k_2, k_3, and k_4 (Table 1) and the relative contributions of A, B, and C to the transient absorption signal as a function of time (Figure 3).

A striking feature emerging from the data fit is that the escape rate from the heme pocket, k_3, competes with the geminate rebinding rate, k_2, in both Mb and HbI. This means that species C, a metastable state in which CN^- is bound to the protein matrix, must be significantly populated in the nanosecond time regime. In fact, by 400 ns the populations of B and C are comparable (Figure 3). In spite of the rapid population of C, the geminate yield is quite high and very few CN^- molecules escape to the solvent. This implies that the escape rate from state C to the solvent, k_5, is much slower than the rate back to state B, k_4, and in turn suggests that the slow overall cyanide dissociation rate (0.011 s^{-1}) may be at least partially controlled by the potential energy barrier between C and D, which may involve the protonation of CN^-. It is not clear if this last step is diffusionally controlled since the proton source is still unidentified, and it is not clear how much of the overall dissociation rate is determined by k_1 and k_5, although one of these must be much smaller than k_3 to achieve the slow overall value of 0.011 s^{-1} (Boffi et al., 1996). As an additional observation, extensive photon pumping creates a photostationary state in which C remains significantly populated on a microsecond to millisecond time scale, thereby increasing the amount of escape of the ligand to the solvent. This mechanism could be at the basis of the reported photolability of the complex under condition of continuous illumination (Keilin & Hartree, 1955; Reddy et al., 1996).

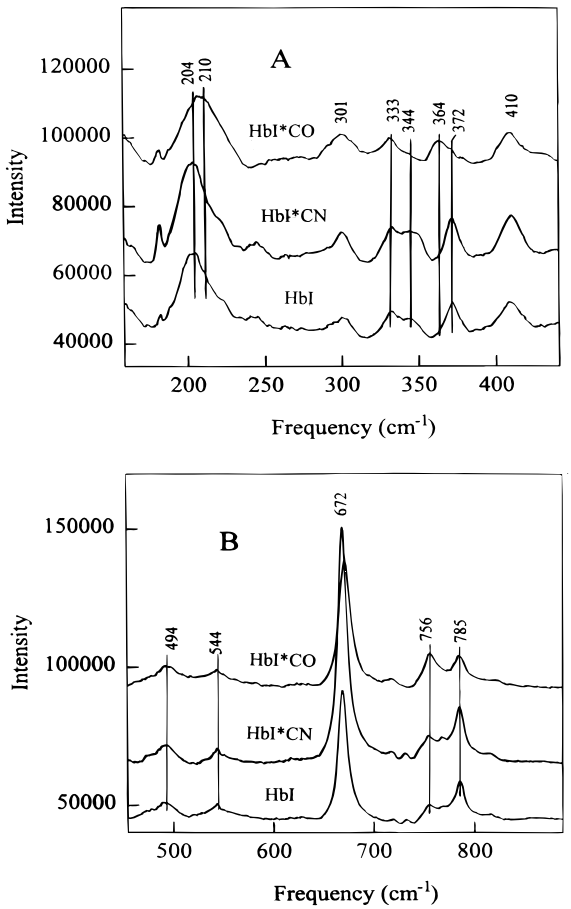

FIGURE 4: 10 ns transient resonance Raman spectra of HbI. Spectra are shown in two distinct frequency regions (A and B). From top to bottom: CO photoproduct (HbI*CO), ferrous cyanide photoproduct (HbI*CN), and deoxy (HbI). The protein concentration was about 0.5 mM in 0.1 M borate buffer at pH 9.2 containing 0.5 M KCN and approximately 2 mM dithionite. The cell path length was 200 μm. The laser wavelength was 435.8 nm, and the laser pulse energy at the sample was approximately 100 μJ.

According to this interpretation, the protonation/deprotonation of cyanide, which is necessary to overcome the protein matrix barrier, must occur while the anion is entering/leaving the C state. The proposed role of the distal histidine as the sole proton source/sink in the transient cyanide protonation (Dou et al., 1996) seems to be unlikely as it would imply a fast escape of cyanidric acid from the protein matrix. It may be envisaged that a second protein residue or a structural water molecule mediates the protonation of the cyanide anion between states C and D.

The analysis of the transient resonance Raman photoproduct of ferrous HbI−CN brings out other unexpected features of the complex that are relevant to the unique mechanism of heme−heme interaction operative in S. inaequivalvis HbI. The spectrum of the 10 ns cyanide photoproduct is identical to that of fully relaxed deoxy HbI (Figure 4) and does not resemble that of the 10 ns CO photoproduct, which was previously shown to undergo tertiary relaxation on the microsecond time scale (Rousseau et al., 1993). In this earlier study, it was observed that the transition from the low-affinity deoxy structure to the high-affinity CO-bound structure was accompanied by changes in the resonance Raman spectrum assigned to modes involving both the heme peripheral substituent groups and the iron−proximal histidine bond. These results are consistent with a previous suggestion that the cooperative interactions are transmitted to a large

extent through the heme propionates (Coletta et al., 1990). This mechanism is in accordance with the high-resolution crystal structures of the CO and deoxy states of HbI (Royer et al., 1989, 1994). The X-ray data also suggest that the destabilization of the subunit interface that leads to the changes in the propionate interactions upon ligand binding is triggered by the expulsion of the Phe 97 phenyl group into the subunit interface. In the deoxy structure, this phenyl group is close to the proximal imidazole. Upon binding of CO, the shift in the proximal histidine as the iron moves into the heme plane is thought to initiate the movement of the phenyl group away from the proximal histidine out into the subunit interface with the concomitant disruption of the hydrogen-bonded water network and the establishment of the new propionate interactions associated with the high-affinity structure (Royer et al., 1994).

The results of the present study show that the 10 ns photoproduct of HbI−CN has the same subunit interface (as reflected in the propionate sensitive modes in the 300−400 cm^{-1} region) and proximal heme pocket (as reflected in the Fe−His stretching mode at 204 cm^{-1}) as the equilibrium deoxy form of HbI. This indicates either that CN^- binding to the ferrous derivative of HbI does not result in the same structural changes that occur when CO binds or that the relaxation pathway of the protein after photolysis is dependent upon ligand identity. The first hypothesis appears to be more realistic in that (i) it is consistent with the cw resonance Raman data (Boffi et al., 1997) which indicate that the spectrum of the ferrous cyanide adduct differs markedly from that of the CO derivative and (ii) if CN^- did induce the same deoxy "T" to liganded "R" transition as CO, the relaxation to the equilibrium deoxy conformation after the ligand−iron bond is broken should occur in the microsecond time scale, i.e., in the time regime of the CO photoproduct relaxation (Rousseau et al., 1993), and hence should be essentially independent of the nature of the ligand.

The critical question now focuses on why CN^- does not induce the same conformational changes in the protein as does CO. An obvious possibility is that the iron does not move into the heme plane upon CN^- binding to the ferrous form. This is not the case, however, as the cw Raman data in the accompanying paper (Boffi et al., 1997) show very clearly that the ferrous cyanide adduct is low spin and that the iron is indeed in the "average" heme plane. However, this does not necessarily imply that the heme itself must be planar. In fact, a distortion of the heme plane involving the N_1 and N_3 pyrrole nitrogen displacement in opposite directions preserves the octahedral symmetry for the iron atom and is compatible with a low-spin state (Boffi et al., 1997). In ferrous cyanide HbI the cw resonance Raman data indicate that, though the adduct is clearly low spin, the υ_4 band (a marker of the π electron density in the heme macrocycle) occurs at a frequency which is more similar to that of the deoxy derivative than to that of the CO-bound derivative, indicating that cyanide binding causes negligible perturbations of the π porphyrin system. In contrast, the binding of CO, NO, or O_2 results in a substantial redistribution of π electron density.

It is proposed that the binding of the cyanide ion to ferrous heme is dominated by σ bonding and that the π back-bonding that occurs with CO or O_2 is very small in magnitude. The effect on the charge density in the iron−proximal histidine bond and on the orientation of the imidazole ring of the proximal histidine with respect to the heme plane is expected to be dramatic because the π overlap between the imidazole ring and the porphyrin ring is thought to be an important source of configurational stability (Scheidt et al., 1986). It may be envisaged that, for cyanide-bound ferrous HbI, the proximal imidazole can be stabilized in a configuration that does not force the phenylalanine (Phe 97) ring into the subunit interface, perhaps involving a lengthened iron−proximal histidine bond, whereas for the more typical diatomic ligands, the electronic interactions favor an imidazole orientation that precludes having the phenyl ring remain near the proximal histidine. If the phenyl ring stays near the heme, none of the more extensive cooperative interactions involved in the T to R conformational change will occur and the CN^- adduct mantains the same configuration as in the deoxy state. Since the cyanide anion binds to the heme iron with only minor modification of the local heme protein structure, the relaxation pathway of the HbI−CN photoproduct can be expected to be very fast (within 10 ns) with no major rearrangements of either the globin or the heme moiety. The primary relaxation processes would be mainly the ballistic movement of iron out of the heme plane and a change in the spin state of the iron [these changes have been shown to occur on a few picosecond time scale in CO, NO, and O_2 photoproducts of HbA and Mb (Petrich et al., 1988)]. Hence, the microsecond relaxation that takes place after the photolysis of CO never occurs after the photolysis of CN^- in that, after 10 ns, the latter photoproduct is in effect already relaxed, and its Raman spectrum corresponds to that of the deoxy species.

REFERENCES

Austin, R. H., Beeson, K. W., Eisenstein, L., Frauenfelder, H., & Gunsalus, I. C. (1975) *Biochemistry 14*, 5355−5373.

Bellelli, A., Antonini, G., Brunori, M., Springer, B. A., & Sligar, S. G. (1990) *J. Biol. Chem. 265*, 18898−18901.

Boffi, A., Chiancone, E., Takahashi, S., & Rousseau, D. L. (1997) *Biochemistry 36*, 4505−4509.

Brunori, M., Antonini, G., Castagnola, M., & Bellelli, A. (1992) *J. Biol. Chem. 267*, 2258-2263.

Chiancone, E., & Gibson, Q. H. (1989) *J. Biol. Chem. 264*, 21062−21065.

Chiancone , E., Vecchini, P., Verzili, D., Ascoli, F., & Antonini, E. (1981) *J. Mol. Biol. 152*, 577−583.

Chiancone, E., Elber, R., Royer, W. E., Regan, R., & Gibson, Q. H. (1993) *J. Biol. Chem. 268*, 5711−5718.

Coletta, M., Boffi, A., Ascenzi, P., Brunori, M. & Chiancone, E. (1990) *J. Biol. Chem. 265*, 4828−4830.

Dou, Y., Olson, J. S., Wilkinson, A. J. & Ikeda Saito, M. (1996) *Biochemistry 35*, 7107−7113.

Gibson, Q. H. (1989) *J. Biol. Chem. 264*, 20155−20158.

Gibson, Q. H., Olson, J. S., McKinnie, R. E., & Rohlfs, R. J. (1986) *J. Biol. Chem. 261*, 10228-10239.

Henry, E. R., Sommer, J. H., Hofrichter, J., & Eaton, W. A. (1983) *J. Mol. Biol. 166*, 443−451.

Keilin, D., & Hartree, E. F. (1955) *Biochem. J. 61*, 153−171.

Petrich, J. W., Poyart, C., & Martin, J. L. (1988) *Biochemistry 27*, 4049−4060.

Reddy, K. S., Yonetani, T., Tsuneshige, A., Chance, B., Kushkuley, B., Stavrov, S. S., & Vanderkooi, J. M. (1996) *Biochemistry 35*, 5562−5570.

Reisberg, P. I., & Olson, J. S. (1980) *J. Biol. Chem. 255*, 4151−4158.

Rousseau, D. L., Song, S., Friedman, J. M., Boffi, A., & Chiancone, E. (1993) *J. Biol. Chem. 268*, 5719−5723.

Royer, W., Jr. (1994) *J. Mol. Biol. 234*, 657−681.

Royer, W., Jr., Hendrickson, W. A., & Chiancone, E. (1989) *J. Biol. Chem. 264*, 21052−21061.

Scheidt, W. R., & Chapman, D. M. (1986) *J. Am. Chem. Soc. 108*, 1163−1647.

BI961889S